Macromolecules

Article

Cite This: Macromolecules 2019, 52, 8114−8123

pubs.acs.org/Macromolecules

Thermal Metamorphosis in (Meth)acrylate Photopolymers: Stress Relaxation, Reshaping, and Second-Stage Reaction

Maciej Podgórski,[†,‡] Brady T. Worrell,[†] Jasmine Sinha,[†] Matthew K. McBride,[†] and Christopher N. Bowman*[,†]

[†]Department of Chemical and Biological Engineering, University of Colorado, UCB 596, Boulder, Colorado 80309, United States

[‡]Department of Polymer Chemistry, Faculty of Chemistry, Maria Curia-Sklodowska University, pl. Marii Curie-Sklodowskiej 5, 20-031 Lublin, Poland

Supporting Information

ABSTRACT: Thermally transformable/responsive (meth)-acrylate photopolymer networks were constructed from commercial (meth)acrylate esters and synthetic di- and mono(meth)acylate monomers bearing thioester functionalities. The thermal responsiveness, here self-limited exchange, relied on the catalytic metamorphosis of thioesters into esters with the concomitant depletion of hydroxyls and subsequent generation of free thiols. The thioester−hydroxyl cross-exchange was demonstrated in network systems with interchain thioesters as well as in networks with side-chain pendant thioacetyls. The interchain metamorphosis resulted in close to 80% conversion of thioesters into esters when 2 equiv of hydroxyl groups was initially present. In practical terms, such an outcome enabled efficient stress relaxation (60%) and good shape adaptation (90% shape fixity) in 1 h at 105 °C. On the other hand, side-chain S → O acyl transfer reactions were found to vary in efficiency depending on the vicinity of thioesters and hydroxyls. When in close vicinity, efficient noncatalytic exchange was observed in materials with 1-to-1 thioester-to-hydroxyl ratios nearing 60%. The benefits of generating free thiols postpolymerization were further explored in enhanced two-stage curing systems where a subsequent thiol−ene photopolymerization was demonstrated at ambient as well as at elevated temperatures.

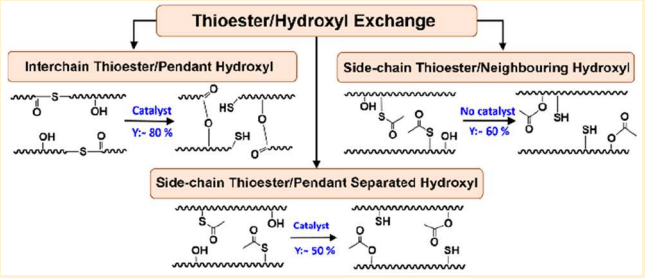

INTRODUCTION

Covalent adaptable networks (CANs) are a unique kind of "enhanced" thermoset materials that, although constructed with covalent building blocks, still possess the ability to flow akin to thermoplastics upon application of an appropriate stimulus. To facilitate viscous flow in CANs requires the inclusion of dynamic covalent chemistry (DCC) and activation of the dynamic chemical reaction.[1−3] Depending on the type of underlying chemistry dictating the mechanism of action, CANs can be divided into three major groups: dissociative, associative, and a third kind of heterogeneous cross-exchange presented here as metamorphosis.[4] Dissociative and associative CANs constitute the majority of dynamic thermoset materials reported to date. The former relies on covalent bonds that revert to their starting reactants, gradually reducing cross-linking density of the network to enable plastic flow while often leading to depolymerization. For example, the Diels−Alder reaction between furan- and maleimide-bearing monomers has been utilized by many researchers in the construction of thermally remendable polymer networks.[5−7] Other notable dynamic reactions adopted in dissociative CANs relay on dynamic breaking of disulfides, alkoxyamines, or thiol−Michael adducts.[8−10]

In contrast, the associative type of CANs maintains constant cross-linking density during the exchange process, in most cases proceeding through the formation of short-lived intermediates that then fragment to return the network to identical, yet displaced chemical connectivity. Here, prominent examples include transesterification,[11] allyl sulfide/thiol exchange,[12] olefin metathesis,[13] boroxine/boronic ester exchange,[14,15] or very recently transthioesterification.[16,17] While dissociative and associative CANs are fully reversible, i.e., every localized dynamic covalent link can be cleaved, displaced, and re-formed *n* number of times, as long as there exists continuous activation, metamorphosis is considered here as an irreversible change usually in both the chemical structure and network connectivity. Metamorphosis is of a self-depleting character and ceases even with continuing stimulation when initial chemical quality (a given type of covalent bonding) is fully transformed into a distinct linkage. Theoretically, any type of AB + C → AC + B reaction could be adopted for this purpose; however, there are obvious practical limitations such as the dynamic units ought likely to be restricted to functionalities

Received: August 9, 2019
Revised: October 4, 2019
Published: October 18, 2019

DOI: 10.1021/acs.macromol.9b01678
Macromolecules 2019, 52, 8114−8123

common in polymer network synthesis and would have to be able to undergo exchange efficiently in solventless conditions.

Therefore, only a few examples of these types of heterogeneous exchange reactions in network systems have been documented so far. For instance, in work by Cooper and co-workers,[18] acrylate resins bearing hindered urea functionalities were first UV polymerized in the presence of alcohol-terminated chain extenders and subsequently conditioned at elevated temperatures which resulted in deblocking of the urea followed by the isocyanate−alcohol reaction (bulky urea−alcohol exchange). This transformation produced a polyurethane and loosely cross-linked polyacrylate with pendant secondary amines (Scheme 1a). In a more recent example, the same strategy was utilized in 3D printing.[19] As before, highly cross-linked and glassy acrylate thermosets were UV-printed at ambient conditions and then postpolymerization heated to deblock urea cross-links that reacted with polyol (or polydiamine) chain extenders to form tough elastomeric 3D constructs. In the whole process, more stable polyurethanes were generated within the initial acrylate matrix, resulting in interpenetrating networks with good toughness. As illustrated in Scheme 1a, many previous examples were limited to an exchange that leads to an overall decrease in cross-linking.

Scheme 1. Schematic Representation of One Example of Metamorphosis within Methacrylate Networks: (a) Previous Reports on Urea−Alcohol/Amine Exchange; (b, c) Current Work on Thioester−Hydroxyl Exchange

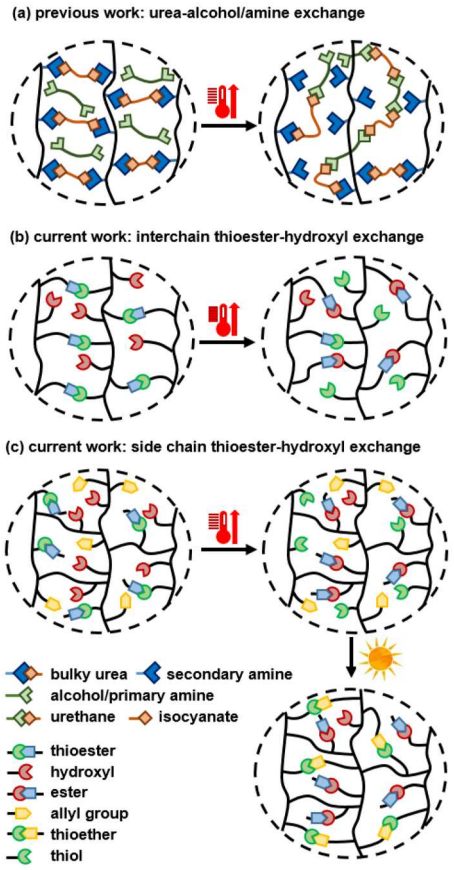

In this study, we assessed the feasibility and benefits of a one-way cross-exchange process between thioesters and alcohols in (meth)acrylate thermosets of various physiomechanical properties. In the present instance, proceeding according to the reaction scheme above, the hybrid exchange between a thioester (AB) and an alcohol (C) would lead to ester (AC) and thiol (B) products which could subsequently be used for various other reactions. More specifically, two general approaches will be described as illustrated in Scheme 1b,c. The first transformation would lead to a material of the same network connectivity (cross-linking density), yet different cross-link character, after exchange. The second transformation would not affect either the density of cross-links or their quality but will be taking place within the network scaffold leading to side group transformations only (Scheme 1c). In addition, those transformations in the structures of pendant chains would be subsequently used to enable second-stage reactions (curing) or functionalization.

EXPERIMENTAL SECTION

Materials. All chemicals and solvents were purchased from commercial suppliers (Sigma-Aldrich, Fisher Scientific, and Bruno Bock) and were used as received without further purification. Initiators: phenylbis(2,4,6-trimethylbenzoyl)phosphine oxide (TPO), 2,2-dimethoxy-2-phenylacetophenone (DMPA), 2,2′-azobis-(2-methylpropionitrile) (AIBN). Reactants and monomers: succinic anhydride, 2-mercaptopropionic acid, 2-hydroxyethyl acrylate (HEA), 2-hydroxyethyl methacrylate (HEMA), hexyl methacrylate (HMA), glycidyl methacrylate, thioacetic acid, potassium thioacetate, allyl alcohol, 2-bromoethanol, acryloyl chloride, methacryloyl chloride, trimethylolpropane triacrylate (TMPTA), allyl acrylate (AA), allyl methacrylate (AMA), trimethylolpropane tris(3-mercaptopropionate) (TMPTMP), *N*,*N*′-diisopropylcarbodiimide (DIC), *p*-toluenesulfonic acid monohydrate (TsOH−H_2O). Organic catalysts: triethylamine (TEA), pyridine, 4-(dimethylamino)pyridine (DMAP), 4-methoxypyridine (4MP), 2-methoxypyridine (2MP), 4-*tert*-butylpyridine (TBP), 4-(trifluoromethyl)pyridine (TFP), imidazole, 1,1,3,3-tetramethylguanidine (TMG). The structures of monomers used in photocurable compositions are depicted in Scheme 2.

Synthesis of Monomers. (i) The thioester dicarboxylic acid (TE) was synthesized according to a previously reported procedure.[16] Shortly, succinic anhydride was dissolved in anhydrous acetonitrile and pyridine (1.00 M total concentration, 9:1 v/v ratio, MeCN:pyridine). Then, an equivalent amount of 3-mercaptopropionic acid was added in a single portion followed by 5.00 mol % of DMAP. The reaction was kept under air and stirred at room temperature overnight (~12 h). After this period the reaction mixture was concentrated and dissolved in ethyl acetate (EtOAc), acidified with a 1 M aqueous HCl solution, and the aqueous layer was extracted with additional portions of EtOAc. Then, the organic phases were dried over Na_2SO_4, filtered, and concentrated (~90% yield).

(ii) The di(meth)acrylate thioesters (DMTE and DATE) were synthesized from TE by adopting the previously reported procedure.[16] To a 250 mL round-bottomed flask equipped with a magnetic stir bar was added 5.0 g (24.3 mmol, 1.00 equiv) of TE1, 535 mg (2.43 mmol, 0.1 equiv) of 2,6-di-*tert*-butyl-4-methylphenol (BHT), and 80 mL of DCM. Next, 148 mg (1.22 mmol, 0.05 equiv, 5.0 mol %) of DMAP, 232 mg (1.22 mmol, 0.05 equiv, 5.0 mol %) of TsOH−H_2O, and 5.0 mL (5.08 g, 43.7 mmol, 1.8 equiv) of 2-hydroxyethyl acrylate were added. Finally, 8.37 mL (6.75 g, 53.5 mmol, 2.2 equiv) of DIC was added via syringe. The suspension was allowed to stir at ambient conditions overnight. After this period the reaction mixture was filtered with EtOAc, and the filtrate was concentrated to give a milky residue. The residue was again suspended in EtOAc (20 mL) and filtered, the filter cake was washed with additional EtOAc, and the filtrate was reduced to yield a clear residue. The residue was submitted to column chromatography (50% EtOAc/hexanes). The exact procedure was utilized to synthesize the thioester dimethacrylate with no changes other than switching HEA for HEMA.

DOI: 10.1021/acs.macromol.9b01678
Macromolecules 2019, 52, 8114−8123

Scheme 2. Chemical Structures of Monomer Used in Three Types of Compositions[a]

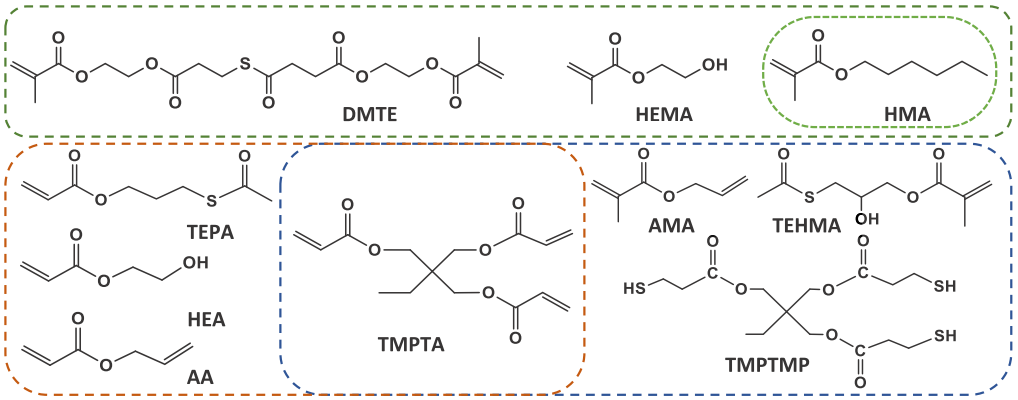

[a]Green dashed lines: methacrylate network components with interchain thioester and pendant hydroxyl (HMA used in control nondynamic material). Blue dashed lines: acrylate network components with side-chain thioester and hydroxyl. Brown dashed lines: (meth)acrylate network components with side-chain thioester and hydroxyl in close vicinity (TMPTMP's role is to reduce the cross-linking density of first-stage network and lower the T_g).

DATE: 98% yield; slightly viscous, clear oil; R_f = 0.45 (TLC conditions: 50% EtOAc/hexanes). ^{1}H NMR (400 MHz, $CDCl_3$, 25 °C): δ = 6.46 (dd, J = 17.3, 1.35 Hz, 2H), 6.16 (dd, J = 17.3, 10.4 Hz, 2H), 5.91−5.88 (m, 2H), 4.40−4.34 (m, 8H), 3.15 (t, J = 7.0 Hz, 2H), 2.91 (t, J = 6.8 Hz, 2H), 2.69 (d, J = 24.7 Hz, 4H). ^{13}C NMR (100 MHz, $CDCl_3$, 25 °C): 197.43, 171.77, 171.47, 165.99, 165.98, 131.65, 131.63, 128.04, 62.63, 62.57, 62.25, 62.24, 38.38, 34.31, 29.06, 24.00.

DMTE: 96% yield; slightly viscous, clear oil; R_f = 0.3 (TLC conditions: 30% EtOAc/hexanes). ^{1}H NMR (400 MHz, $CDCl_3$, 25 °C): δ = 6.16−6.14 (m, 2H), 5.63−5.61 (m, 2H), 4.60−4.57 (m, 4H), 4.38−4.35 (m, 8H), 3.15 (t, J = 7.01 Hz, 2H), 2.91 (t, J = 7.18 Hz, 2H), 2.72−2.66 (m, 4H), 1.97 (s, 6H). ^{13}C NMR (100 MHz, $CDCl_3$, 25 °C): 197.41, 171.77, 171.47, 167.22, 167.21, 135.99, 126.30, 126.18, 118.66, 62.64, 62.58, 62.42, 62.42, 38.40, 34.34, 29.08, 24.02, 18.43.

(iii) 3-Hydroxypropyl thioacetate was synthesized in a one-step procedure from allyl alcohol and thioacetic acid. Allyl alcohol (2 g, 0.034 mol) was mixed with 3.93 g (0.052 mol) of thioacetic acid followed by the addition of 0.06 g (0.4 mmol) of AIBN. The reaction mixture was kept stirring at 70 °C for 1 h. Then, the crude product was directly subjected to column chromatography to give clear liquid. Yield: 82%. ^{1}H NMR ($CDCl_3$, 25 °C): δ = 3.59 (t, J = 7.11 Hz, 2H), 2.95 (t, J = 8.2 Hz, 2H), 2.29 (s, 3H), 1.77 (m, 2H). ^{13}C NMR ($CDCl_3$): 197.2, 60.3, 32.3, 30.5, 25.5.

(iv) 3-(Acetylthio)propyl acrylate (TEPA) was synthesized from 3-hydroxypropyl thioacetate and acroyoyl chloride. To the solution of 5 g (0.037 mol) of thioacetic ester in 30 mL of anhydrous DCM, 4.2 g (0.041 mol) of TEA was added at 0 °C under a nitrogen atmosphere. Then, 3.7 g (0.041 mol) of acryloyl chloride in 5 mL of anhydrous DCM was added dropwise at 0 °C. After the completion of the addition, the reaction mixture was stirred overnight at room temperature under a nitrogen atmosphere. The organic layer was then washed with $NaHCO_3$ followed by washing with brine and DI water. The combined organic layers were dried over Na_2SO_4 and concentrated to give pale yellow liquid. The crude product was purified by column chromatography (silica gel, hexane/EtOAc 55:45) to obtain a colorless liquid. Yield: 55%. ^{1}H NMR ($CDCl_3$): δ = 6.42 (dd, J_1 = 17.05 Hz, J_2 = 2.09 Hz, 1H), 6.15 (dd, J_1 = 17.22 Hz, J_2 = 10.4 Hz, 1H), 5.85 (dd, J_1 = 10.43 Hz, J_2 = 1.66 Hz, 1H), 4.23 (t, J = 6.03 Hz, 2H), 2.98 (t, J = 7.82 Hz, 2H), 2.36 (s, 3H), 1.98 (m, 2H). ^{13}C NMR ($CDCl_3$): 195.56, 166.10, 130.97, 128.28, 62.89, 30.63, 28.67, 25.67.

(v) 3-(Acetylthio)-2-hydroxypropyl methacrylate (TEHMA)[20] was synthesized according to a previously reported procedure. Shortly, in methylene chloride solution thioacetic acid (1.8 g, 22 mmol) and glycidyl methacrylate (20 mmol) were reacted in the presence of TEA (1 mmol) for 10 h at room temperature. After this period, the mixture was washed with 1 M HCl aqueous solution, saturated $NaHCO_3$, and DI water and dried over anhydrous Na_2SO_4. After solvent removal, TEHMA was obtained in good yield (~90%). ^{1}H NMR ($CDCl_3$, 25 °C): δ = 6.16 (s, 1H), 5.62 (s, 1H), 4.22 (m, 2H), 4.04 (m, 1H), 3.02−3.22 (m, 2H), 3.02 (b, 1H), 2.38 (s, 3H), 1.97 (s, 3H). ^{13}C NMR ($CDCl_3$): 196.24, 167.38, 135.81, 126.38, 69.17, 67.01, 32.61, 30.57, 18.33.

Composition Preparation. The compositions were prepared from the monomers depicted in Scheme 2 where the structures are grouped in a composition-wise manner.

The interchain thioester network was composed of DMTE (1 M), HEMA (2 M), DMAP (3 mol % with respect to thioester content), and UV-sensitive photoinitiator DMPA (0.2 wt %). Curing was performed by 10 min exposure to UV light of 10 mW/cm^2 (365 nm).

The interchain thioester control network contained DMTE (1 M), HEMA (2 M), HMA (0.2 M), and a UV-sensitive photoinitiator DMAP (0.2 wt %). The curing procedure was the same as above.

Side-chain thioester acrylate networks were composed of four primary components: TEPA/HEA/AA/TMPTA were used in molar ratios of 1.5 M/1 M/1 M/0.1 M. The DMAP concentration was 5 mol % with respect to the thioester monomer. DMPA and TPP were used at 0.2 wt % each. The first-stage curing was performed at ambient conditions by 10 min exposure to visible light of 20 mW/cm^3 (400−500 nm). Second-stage curing was performed for 10 min with UV light of 50 mW/cm^2 (320−390 nm).

Side-chain thioester (meth)acrylate networks were made of the four components TEHMA/AMA/TMPTA/TMPTMP used in molar ratios 1 M/2 M/0.1 M/0.2 M. If used, the DMAP concentration was 5 mol % relative to the thioester monomer. DMPA and TPP were used at 0.2 wt % each. The first-stage curing was performed as described above. Second-stage curing was performed at ambient temperature (or at 60 °C) for 10 min with UV light of 50 mW/cm^2 (320−390 nm).

Material Characterization. *Fourier Transform Infrared Spectroscopy.* Photopolymerization kinetics were analyzed by using an FT-IR spectrometer (Nicolet 8700). The functional group conversions were analyzed in real time in the transmission mode. Resins were sandwiched between glass slides separated with 250 μm spacers and placed into a horizontal transmission apparatus where they were photocured with either UV light of 10 mW/cm^2 (365 nm) or visible light of 20 mW/cm^2 (400−500 nm). The final resin conversions were calculated from the absorbance peak area of the vinyl functional group, around 6150 cm^{-1} in the near-infrared spectrum. Hydroxyl and thioester carbonyl conversions were analyzed in the ATR-IR mode. Photocured samples of fixed geometries (5 mm/15 mm/0.25 mm) were surface-analyzed in ATR-IR where the highest peak absorbance

DOI: 10.1021/acs.macromol.9b01678
Macromolecules 2019, 52, 8114−8123

was set to 0.9−1. After thermal annealing (metamorphosis) for 30 min, 1, 2, 3, 4, 5, 10, or 20 h the samples were placed in the ATR-IR and scanned in the mid-IR range (650−4000 cm^{-1}). The metamorphosis extent was estimated from hydroxyl conversions by monitoring the decrease in the OH signal at 3480 cm^{-1}. Concomitantly, the thioester conversion was analyzed by deconvoluting the thioester carbonyl signal at 1690 cm^{-1} from the ester carbonyl signal at 1720 cm^{-1}. Deconvolution was performed using Fityk software[21] (version 1.3.1) where IR peaks were assumed to have Gaussian distribution functions. Neither technique offers high accuracy in the conversion assessment as hydroxyls exhibit broad signal due to the hydrogen bonding which would underrepresent the real conversion values. On the other hand, the carbonyl group signal shifts and widens after polymerization, which is expected to misrepresent the absolute values as well. However, when combined together, both methods complement themselves and affirm the overall estimates. Generally, the difference between values from both methods coincided well and varied by no more than 10%.

Dynamic Mechanical Analysis (DMA) and Stress Relaxation. The glass transition temperature (T_g) and storage modulus (E') were determined on a Q800 DMA (TA Instruments) by using a ramp rate of 3 °C/min and a frequency of 1 Hz, with a fixed oscillatory strain of 0.02%. Stress relaxation experiments were performed in tensile elongation by using a Q800 DMA instrument. The built-in stress relaxation DMA settings were used, with a 5% maximal strain, and an initial strain rate of 1%/min at a given temperature. Rectangular samples of the dimensions 10/4−5/0.25 mm were measured with calipers prior to testing.

RESULTS AND DISCUSSION

Interchain Thioester/Side-Chain Hydroxyl Exchange. Reactions of thioesters, such as cleaving of the thioester bond and acyl transfer, are well-known processes that are regularly employed, i.e., in peptide and protein biomacromolecule synthesis and coupling.[22,23] Notably, many of other acyl transfer reactions involving thioesters and esters, such as acyl N → S shift or S → N, O → N, O → O, and S → S, are all omnipresent in the field of biochemistry and bioengineering, with particular emphasis on the native chemical ligation and its multiple variations.[24−28] Motivated by the recent reports on associative dynamic materials based on transthioesterification[17,29,30] where the thiol functionality allowed for very efficient and repeatable thiol−thioester exchange (acyl S → S shift) at ambient temperatures in the presence of weak bases, we decided to expand on the subject and investigate thioester-based methacrylate thermoset materials capable of undergoing metamorphosis. By adopting the previous synthetic approach, a di(meth)acrylate thioester monomer in which the thioester functionality resides between two (meth)acrylate double bonds was synthesized in analogy to the previously synthesized diallyl compound[16] (Scheme 2). Copolymerization of the dimethacrylate thioester (DMTE) with a monomethacrylate such as hydroxyethyl methacrylate (HEMA) yielded a glassy thermoset where every cross-linking unit is connected through the thioester. Thus, every cross-link could be potentially cleaved and re-formed provided that the reaction of the thioester with pendant hydroxyl groups occurs. To increase the probability of such cross-exchange, a 2-fold molar excess of hydroxyl groups was used with respect to the thioester content. The radical photo-copolymerization of DMTE (1 M) and HEMA (2 M) in the presence of an exchange catalyst (DMAP) used in the amount of 3 mol % with respect to the thioester yielded a thermoset with a glass transition temperature of 105 °C. To contrast the properties of this material with a nondynamic equivalent, a control composition was prepared comprising DMTE (1 M), HEMA (2 M), and hexyl methacrylate (0.2 M). The use of hexyl methacrylate (HMA)—acting as plasticizer here—was dictated by the significantly higher T_g of the neat DMTE/HEMA sample compared with analogous samples containing DMAP. Incorporating HMA allowed for identical samples in terms of thermomechanical response (see DMA second runs in Figure S1). Metamorphosis, assumed to proceed through a two-step addition/elimination process (nucleophilic acyl substitution) in resemblance to the mechanism detailed for nucleophile-catalyzed thioester−thiol exchange, was triggered thermally by bringing the samples to the glass transition, i.e., close to 105 °C or above. Initial attempts involved using imidazole as the catalyst, as it was proven effective in peptide functionalization.[31,32] However, it turned out to be ineffective here—minimal metamorphosis was observed even at temperatures nearing 200 °C. To monitor the extent of thioester−alcohol exchange in methacrylate thermosets, rectangular specimens annealed at elevated temperatures were assessed in ATR FT-IR. The hydroxyl as well as thioester carbonyl signal depletion was indicative of the exchange progress (Figure 1).

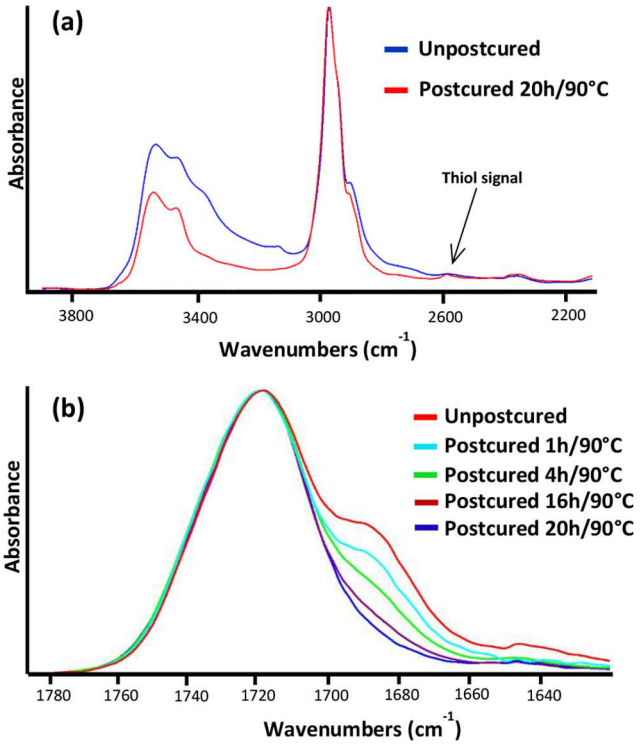

Figure 1. ATR-IR partial scans depicting relevant functional group signals (OH, SH, CO ester, and CO thioester) for dimethacrylate thioester−2-hydroxyethyl methacrylate photopolymers. Evident is reduction in the OH signal and appearance of SH signal (a) as well as gradual disappearance of CO thioester signal (b) with the thermal metamorphosis over time.

Other pyridine derivatives were also assessed for their catalytic abilities (Table 1). However, DMAP has proven to be the most suitable for this purpose, as it is nonvolatile and apparently has higher affinity for the carbonyl groups than the volatile liquid pyridines. It enables good control over the exchange reaction at moderate temperatures with good efficiencies (close to 80% conversion was noted in samples postcured for 20 h at 90 °C or 2 h at 105 °C). Initially, TMG

DOI: 10.1021/acs.macromol.9b01678
Macromolecules 2019, 52, 8114−8123

Table 1. Catalyst Efficiency Studies in Nucleophilic Acyl Substitution in Dimethacrylate Networks[a]

catalyst	heating time/ temp	hydroxyl conv (%)	indirect thioester conv based on OH conv (%)	thioester conv from peak deconvolution (%)
imidazole	2 h/200 °C	30 (3)	60	
TMG[b]	10 min/ambient	50 (−)	100	100 (−)
DMAP	20 h/90 °C	38 (1)	76	80 (6)
DMAP	2 h/90 °C	28 (4)	56	57 (5)
DMAP	5 min/150 °C	16 (3)	32	
DMAP	15 min/120 °C	19 (3)	38	
4MP	3 h/150 °C	13 (3)	26	19 (3)
2MP	3 h/150 °C	9 (4)	18	25 (4)
TBP	3 h/150 °C	11 (3)	22	39 (5)
TFP	3 h/150 °C	18 (3)	36	43 (1)

[a]3 mol % of the catalyst was used with respect to the thioester content. The hydroxyl/thioester ratio was set to 2/1. Standard deviation values are included in parentheses. [b]Initial experiments performed using mixtures of diacrylate thioester (DATE) and 2-hydroxyethyl acrylate.

was also tested in a mixture of diacrylate thioester with hydroxyethyl acrylate. TMG catalyzed the exchange rapidly at ambient conditions followed by subsequent thiol−Michael addition as an undesired side reaction (Figure S2). Lack of control over the exchange precluded its further use. To characterize the dynamic nature of the thioester networks, DMA and stress relaxation experiments were performed. The storage and loss moduli as well as the damping factors (tangent δ) were estimated in unannealed, 100% active thioester and thermally annealed materials with roughly 30 and 60% of reacted thioesters. For comparison, a catalyst-free 100% thioester exchange inactive material was tested. Because the evolution of mechanical properties was inherently initiated in these materials during the analysis, therefore first and second DMA runs were collected and compared. The DMA data are presented in Figures 2a−d. It was not expected that the metamorphosis would cause any significant differences in the cross-linking densities, and indeed the rubbery moduli for all materials tested exhibited similar range during and after exchange (25−45 MPa). These difference likely result from thermal postcuring rather than exchange which is more significant for the samples postprocessed early after curing when there are still active radicals trapped in the networks. Second DMA runs reveal no further change in rubbery moduli values, even though the thioester−OH exchange would still be possible to an extent. From the first DMA scans (Figures 2a,b), it is evident that the exchange reaction initially adds to the material inhomogeneity as the loss modulus results in a broad shoulder for an unannealed, 100% active thioester material and a broad peak for 70% active thioester material. Similarly, the tangent delta profiles show characteristic evolution of two overlapping transitions which at sufficiently high conversions merge into one single transition (Figures 2c,d). Only the materials with significant concentrations of both types of cross-links ("stiffer" ester and "softer" thioester) temporarily exhibit these broadened relaxations. Such behavior seems to preclude any phase or microphase separation in these systems because after sufficient exchange they transform into uniform, single relaxations as observed for predominantly thioester-cross-linked and/or ester-cross-linked networks.

Accordingly, to visualize the extent and ability of reshaping, the materials were annealed thermally for a prescribed amount of time in an undeformed state, thus depleting some of the thioester functionalities without dimensional shape change. Then, the samples were deformed and exposed to heat again to observe the extent of shape adaptation when only a limited

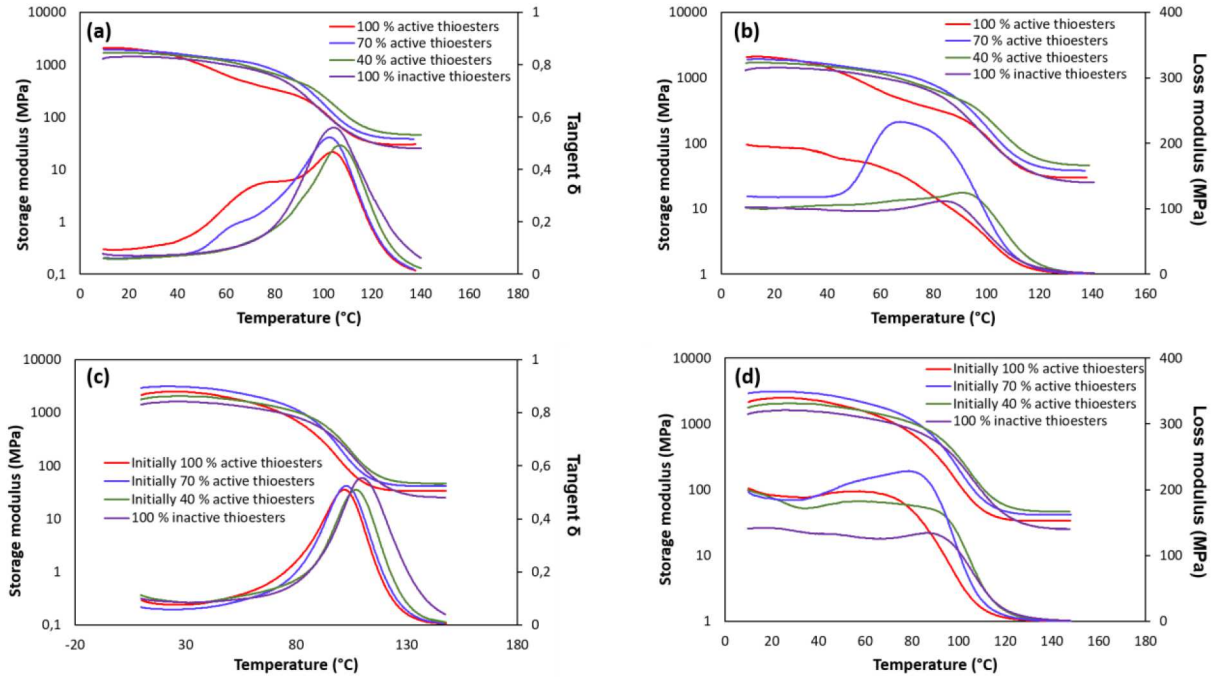

Figure 2. DMA profiles for the interchain thioester methacrylate networks with exchange active thioesters when catalyst DMAP is present (3 mol %) and thioester control without catalyst (exchange inactive thioesters). First DMA scans of storage modulus, loss modulus, and tangent δ (a, b). Second DMA runs (c, d).

DOI: 10.1021/acs.macromol.9b01678
Macromolecules 2019, 52, 8114−8123

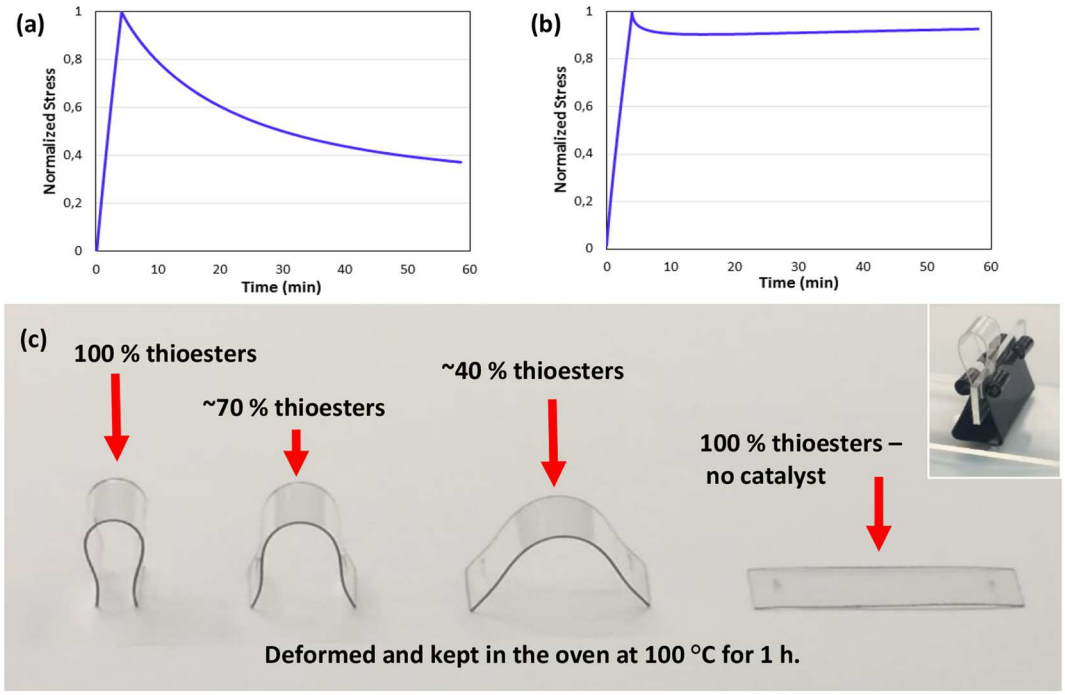

Figure 3. DMA stress relaxation profiles in interchain thioester methacrylate networks (a) with and (b) without catalyst DMAP. Reshaping experiments performed on samples with varied initial interchain thioester content (c).

number of cleavable cross-links still persist in the otherwise nondynamic scaffold. The results are summarized in Figure 3.

From Figure 3a, over 60% stress reduction in 1 h can be seen at 105 °C in materials containing DMAP. On the other hand, no significant stress reduction in the control system can be seen, other than initial (<10%) and fully reversible pseudoplastic stress drop (Figure 3b). In addition, 2 h stress relaxation experiments lead to around 70% stress reduction (Figure S3) which coincides well with the maximal conversions measured in this system (Table 1). As expected, the ability of reshaping varies greatly depending on the thioester concentration (Figure 3c). A material with 100% cleavable cross-links adapts to a new shape with close to 90% shape fixity which deteriorates significantly in samples containing reduced levels (70 and 40%) of the active cross-links. An unannealed, 100% thioester sample, but without DMAP, shows 0% shape fixity at the given conditions, recovering completely to its original shape. Interestingly, 90% shape fixity may suggest higher reaction yield compared to what was measured in unstrained samples annealed for a longer time (Table 1). On the other hand, such efficient reshaping is suggestive of an insignificant extent of side reactions that would lead to permanent cross-links, such as e.g. undesired transesterification which would cause permanent cross-linking and lead to an inability to reshape the material. It is hypothesized also that the metamorphosis is facilitated by thiol−thioester exchange as the probability of transthioesterification would increase initially with thioester conversion. After initial metamorphosis, thioesters can dislocate within the network while engaging in reactions with increasing concentration of free thiols. Once the thioester exchanges with a hydroxyl group, the new ester position becomes permanently locked.

Side-Chain Thioester/Side-Chain Hydroxyl Exchange. In our second approach, the thioester−hydroxyl exchange in networks of fixed cross-linking densities was assessed. As these transformations would affect only the pendant functionalities, the metamorphosis was not expected to introduce significant mechanical changes within the networks themselves. Two composition variations were tested: one primarily based on acrylates and another on methacrylates. Both systems comprised four monomer mixtures and slightly varied in first-stage glass transition temperatures. One fundamental difference was having thioesters either separated from hydroxyls or in close vicinity to hydroxyls. The first system was achieved by copolymerization of bifunctional acrylate thioester monomer with hydroxyl ethyl acrylate. The second system comprised a trifunctional monomer in which the thioester is separated from the hydroxyl by an ethylene group, i.e., 3-(acetylthio)-2-hydroxypropyl methacrylate (Scheme 2). In both systems TMPTA was used as the cross-linker. Also, allyl acrylate or allyl methacrylate were added and served as carriers of double bonds rich in electrons. Details on the exact compositions are found in the Experimental Section. Radical homopolymerization of allyl acrylate results in a significant amount of allyl double bonds left unreacted after the polymerization process (Figure S4). Deconvolution of the double-bond overtone signals results in estimates of 90% acrylate and 40% allyl conversions. The goal was to cure the first-stage resin in radical photo-copolymerization of (meth)-acrylates and preserve a sufficient amount of unreacted allylic functional groups for second-stage thiol−ene photopolymerization with the released thiols. To achieve this aim, two orthogonal photoinitiators were used, namely UV-active DMPA and visible-light-absorbing TPOP. In the first system comprising thioesters at a distance from hydroxyls, a 0.5 molar excess of thioesters was used. The metamorphosis (acyl transfer to hydroxyl groups) was again monitored with ATR-IR. As the thioester concentration was substantially higher than in previous DMTE copolymerizations, transmission IR spectra were also collected to observe the increasing amount of

DOI: 10.1021/acs.macromol.9b01678
Macromolecules 2019, 52, 8114−8123

deprotected thiols over time (Figure 4). Uniquely, such a kind of metamorphosis can be regarded as a solventless thiol

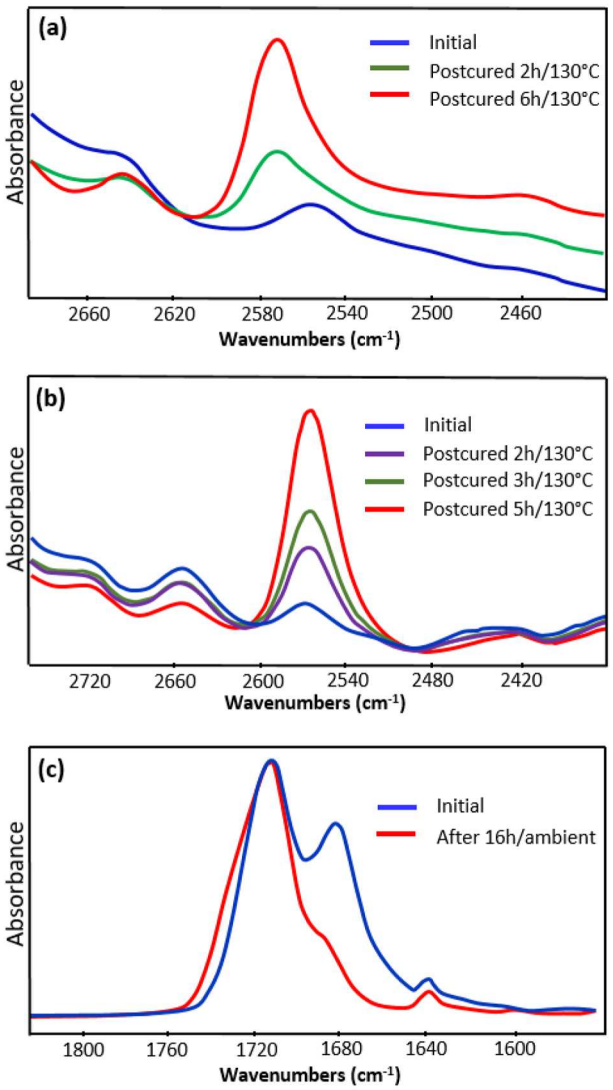

Figure 4. FT-IR spectra collected after fixed time intervals followed thermal metamorphosis. Catalytic side-chain metamorphosis in acrylate system where pendant thioesters are separated from hydroxyls results in 50% hydroxyl conversions with concomitant thiol release (a). Noncatalytic side-chain metamorphosis in methacrylate system where thioesters are in close vicinity with hydroxyls results in 55−60% conversions of hydroxyls with concomitant thiol generation (b). Catalytic side-chain metamorphosis in methacrylate system results in room temperature metamorphosis overnight leading to 65% hydroxyl and thioester conversions (c).

deprotection within the network scaffold. Although used in excess, thioester acyl transfer along the pendant chains was not as efficient as in previous experiments on interchain-located thioesters. The maximal hydroxyl conversion was measured to be around 50%, implying thioester conversion of around 30%. Additionally, the thioester carbonyl peak deconvolution results in around 35−40% thioester conversion, which is in good agreement with IR-measured OH conversions (exemplary deconvolution profiles are included in Figure S5). These ceiling conversions were achieved by thermally annealing the samples for 5−6 h at 125−135 °C. Any longer processing, or processing at higher temperatures, initiates the second-stage curing of the thiols and enes. This behavior is presumed to happen spontaneously and/or by radical initiation through thermal cleaving of the photoinitiator, DMPA. Neither other reaction occurs substantially when metamorphosis is interrupted earlier, i.e., after <6 h at around 130 °C. As a proof of concept demonstration, a reshaping experiment was attempted for the side-chain thioester acrylate material, in analogy to the one for the interchain thioester methacrylate network. Because the peripheral metamorphosis does not affect the mainframe of the network scaffold, only minimal shape adaptation was achieved after thermal postprocessing (see Figure S6). For the case of the second system incorporating thioesters and hydroxyl in close vicinity to each other, the presence of an exchange catalyst (DMAP) facilitates the reaction at ambient conditions and leads to 65% conversion (based on hydroxyl peak signal) or 61% conversion as assessed from thioester carbonyl peak deconvolution after overnight sample storage (Figure 4c and Figure S7).

Unfortunately, the ambient activation results in no control over the exchange process. However, catalyst-free samples can still be thermally reprocessed to achieve good conversion in otherwise stable networks (Figure 4b). By determining the upper time/temperature limitations of thermal metamorphosis in the acrylate system, 5 h of annealing at 130 °C was implemented for the methacrylate system which resulted in conversions of around 55−60%.

Additional thermal postprocessing does not improve the reaction yield and increases the risk of spontaneous thiol−ene cross-linking. After establishing the optimal conditions for side-chain metamorphosis, the second-stage thiol−ene curing was subsequently attempted. Overall, the processing of the resins involved three steps: (i) photopolymerization of the monomer mixture by visible light irradiation in the presence of TPO (0.2 wt %); (ii) thermal metamorphosis to convert terminal thioesters into esters and release thiol groups (typically performed for 5 h at 130 °C); (iii) thiol−ene cross-linking by UV exposure in the presence of 0.2 wt % DMPA.

Such two-stage curable materials constitute an interesting variation to the previously reported thiol−(meth)acrylate resins where the thiol−ene reaction (thiol−Michael addition) was performed in the first step followed by acrylate or methacrylate homopolymerization.[33−35]

In either system the second-stage curing was conducted for 10 min with UV light exposure of 50 mW/cm^2 (320−390 nm). Because of the higher glass transition temperature of the methacrylate system (35 °C) as compared with the acrylate one (16 °C), the curing was also performed at 60 °C.

The second-stage kinetic and DMA results are included in Figures 5 and 6. As can be seen, the thermal metamorphosis only slightly changes the thermomechanical profiles of either type of material. There are minor shifts in glass transitios and/or an insignificant increase in rubbery plateau modulus after thermal annealing and acyl transfer reactions. Little change in the thermomechanical properties is expected, though methacrylate and acrylate thermal postcuring is also possible to an extent, even though these were relatively loosely cross-linked low T_g systems.

As there is enough mobility in the thioester acrylate first-stage network after metamorphosis which is still rubbery at ambient temperature (T_g = 20 °C), the second-stage thiol−ene reaction leads to significantly higher conversions and hence enhanced material properties. Around 50% of the released

DOI: 10.1021/acs.macromol.9b01678
Macromolecules 2019, 52, 8114−8123

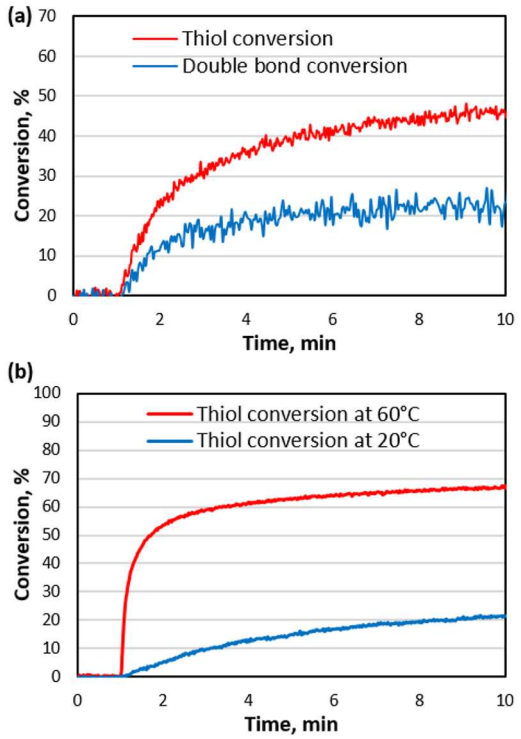

Figure 5. Second-stage conversion analysis after side-chain metamorphosis for acrylate system (a) and methacrylate system (b). In predominantly methacrylate-based noncatalytic system the curing was also performed at 60 °C to account for its glassy nature and to induce additional chain mobility and hence reaction conversion.

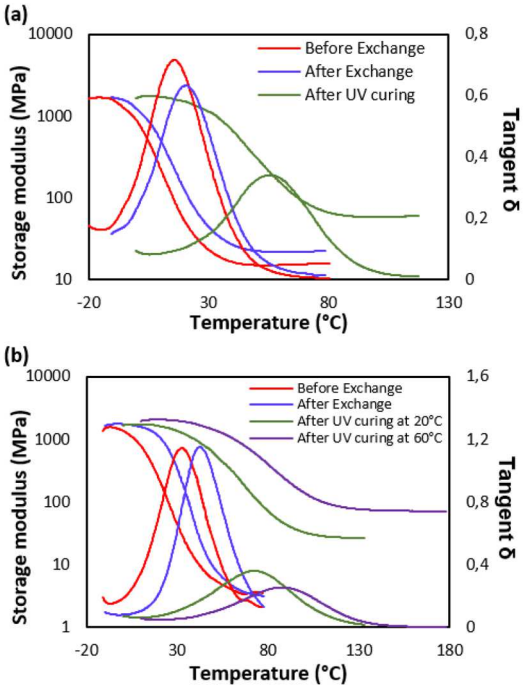

Figure 6. DMA results for (a) acrylate and (b) methacrylate two-stage photopolymers with the ability for peripheral metamorphosis. Included is data on sample before exchange, after thermal processing, and after second-stage curing.

thiols were reacted with allylic functional groups. At the same time conversion of the latter functionalities was measured to be between 20 and 30%. The second-stage curing increased the T_g from 20 to 57 °C and the rubbery plateau by 4-fold (Figures 5a and 6a). On the other hand, the methacrylate system exhibited higher T_g which still increased after metamorphosis to 42 °C. In such a glassy material, because of mobility restrictions, the ambient curing results in low thiol conversions (around 20%). However, when polymerized at 60 °C, the thiol conversion increased to 65% (Figure 5b). Moreover, the increase in cross-linking after second-stage curing leads to more elastic networks below the glass transition as denoted by lower tangent δ values, suggesting less damping below T_g (Figures 6a,b). Such phenomena, less apparent in interchain thioester networks, were recently studied in thiol−ene systems of diverse structural morphologies.[36] Additional DMA data showing the evolution of the loss modulus in both acrylate and methacrylate systems is included in Figure S8. A broadening trend in the transition was also observed in striking analogy to the tangent δ profiles presented in Figure 6. Although microphase separation cannot be completely ruled out in these complex multicomponent systems, the broadening of the relaxations here is attributed to the increase in cross-linking after the second-stage UV curing as well as the introduction of a new type of "softer" sulfide cross-links. Overall, it has to be emphasized that contrary to classic two-stage systems, the current approach allows for extended control over the second-stage curing which could be manipulated pertaining to the application needs. The amount of released thiols can be varied with time/temperature of metamorphosis and so can be the extent of second-stage thiol−ene polymerization.

CONCLUSIONS

The cross-exchange between thioesters and hydroxyls was explored in two types of (meth)acrylate cross-linking systems. It was found that interchain metamorphosis allows for facile conversion of more labile "softer" thioesters into more stable "stiffer" esters with concomitant consumption of hydroxyls and deblocking of thiols. Such transformations enable one-time stress relaxation and shape adaptation in glassy (meth)acrylate thermosets. In addition, two-stage photopolymerization systems were also designed in which metamorphosis did not alter the first-stage network architecture but enabled second-stage thiol−ene reaction. Two variations of such systems were analyzed, i.e., metamorphosis was triggered either catalytically or noncatalytically depending on the vicinity of pendant thioesters and hydroxyls. The findings reported are of practical significance in the design of smart thermoset materials for use in coatings, holography, 3D printing, and so on. As a whole, metamorphosis not only presents a unique ability to permanently change the structure and properties of a given thermoset material but also offers the opportunity for subsequent transformations as evidenced here in the second-stage curing.

ASSOCIATED CONTENT

Supporting Information

The Supporting Information is available free of charge on the ACS Publications website at DOI: 10.1021/acs.macromol.9b01678.

DMA storage moduli, loss moduli and tangent delta, FT-IR and ATR-IR data as well as a reshaping

DOI: 10.1021/acs.macromol.9b01678
Macromolecules 2019, 52, 8114−8123

demonstration on an acrylate side-chain thioester sample (PDF)

AUTHOR INFORMATION

Corresponding Author

*(C.N.B.) E-mail christopher.bowman@colorado.edu.

ORCID

Brady T. Worrell: 0000-0001-7472-2063

Christopher N. Bowman: 0000-0001-8458-7723

Notes

The authors declare no competing financial interest.

ACKNOWLEDGMENTS

This study was supported by the NSF CHE 1808484 and NSF MRSEC (DMR 1420736).

REFERENCES

(1) Zou, W.; Dong, J.; Luo, Y.; Zhao, Q.; Xie, T. Dynamic Covalent Polymer Networks: From Old Chemistry to Modern Day Innovations. *Adv. Mater.* **2017**, *29* (14), 1606100.

(2) Denissen, W.; Winne, J. M.; Du Prez, F. E. Vitrimers: Permanent Organic Networks with Glass-like Fluidity. *Chem. Sci.* **2016**, *7* (1), 30−38.

(3) Zhang, Z. P.; Rong, M. Z.; Zhang, M. Q. Polymer Engineering Based on Reversible Covalent Chemistry: A Promising Innovative Pathway towards New Materials and New Functionalities. *Prog. Polym. Sci.* **2018**, *80*, 39−93.

(4) Mcbride, M. K.; Worrell, B. T.; Brown, T.; Cox, L. M.; Sowan, N.; Wang, C.; Podgorski, M.; Martinez, A. M.; Bowman, C. N. Enabling Applications of Covalent Adaptable Networks. *Annu. Rev. Chem. Biomol. Eng.* **2019**, *10*, 175−198.

(5) Chen, X.; Dam, M. A.; Ono, K.; Mal, A.; Shen, H.; Nutt, S. R.; Sheran, K.; Wudl, F. A Thermally Re-Mendable Cross-Linked Polymeric Material. *Science* **2002**, *295* (5560), 1698−1702.

(6) Scott, T. F.; Bowman, C. N.; Adzima, B. J.; Kloxin, C. J.; Aguirre, H. A. Rheological and Chemical Analysis of Reverse Gelation in a Covalently Cross-Linked Diels−Alder Polymer Network. *Macromolecules* **2008**, *41* (23), 9112−9117.

(7) Reutenauer, P.; Buhler, E.; Boul, P. J.; Candau, S. J.; Lehn, J. M. Room Temperature Dynamic Polymers Based on Diels-Alder Chemistry. *Chem. - Eur. J.* **2009**, *15* (8), 1893−1900.

(8) Amamoto, Y.; Otsuka, H.; Takahara, A.; Matyjaszewski, K. Self-Healing of Covalently Cross-Linked Polymers by Reshuffling Thiuram Disulfide Moieties in Air under Visible Light. *Adv. Mater.* **2012**, *24* (29), 3975−3980.

(9) Jin, K.; Li, L.; Torkelson, J. M. Recyclable Crosslinked Polymer Networks via One-Step Controlled Radical Polymerization. *Adv. Mater.* **2016**, *28* (31), 6746−6750.

(10) Zhang, B.; Digby, Z. A.; Flum, J. A.; Chakma, P.; Saul, J. M.; Sparks, J. L.; Konkolewicz, D. Dynamic Thiol-Michael Chemistry for Thermoresponsive Rehealable and Malleable Networks. *Macromolecules* **2016**, *49* (18), 6871−6878.

(11) Capelot, M.; Montarnal, D.; Tournilhac, F.; Leibler, L. Metal-Catalyzed Transesterification for Healing and Assembling of Thermosets. *J. Am. Chem. Soc.* **2012**, *134* (18), 7664−7667.

(12) Scott, T. F.; Schneider, A. D.; Cook, W. D.; Bowman, C. N. Photoinduced Plasticity in Cross-Linked Polymers. *Science* **2005**, *308* (June), 1615−1617.

(13) Lu, Y. X.; Tournilhac, F.; Leibler, L.; Guan, Z. Making Insoluble Polymer Networks Malleable via Olefin Metathesis. *J. Am. Chem. Soc.* **2012**, *134* (20), 8424−8427.

(14) Leibler, L.; Breuillac, A.; Nicolaÿ, R.; van der Weegen, R.; Röttger, M.; Domenech, T. High-Performance Vitrimers from Commodity Thermoplastics through Dioxaborolane Metathesis. *Science* **2017**, *356* (6333), 62−65.

(15) Brooks, W. L. A.; Sumerlin, B. S. Synthesis and Applications of Boronic Acid-Containing Polymers: From Materials to Medicine. *Chem. Rev.* **2016**, *116* (3), 1375−1397.

(16) Worrell, B. T.; McBride, M. K.; Lyon, G. B.; Cox, L. M.; Wang, C.; Mavila, S.; Lim, C.-H.; Coley, H. M.; Musgrave, C. B.; Ding, Y.; Bowman, C. N. Bistable and Photoswitchable States of Matter. *Nat. Commun.* **2018**, *9* (1), 2804.

(17) Wang, C.; Goldman, T. M.; Worrell, B. T.; McBride, M. K.; Alim, M. D.; Bowman, C. N. Recyclable and Repolymerizable Thiol-X Photopolymers. *Mater. Horiz.* **2018**, *5* (6), 1042−1046.

(18) Velankar, S.; Pazos, J.; Cooper, S. L. High-Performance UV-Curable Urethane Acrylates via Deblocking Chemistry. *J. Appl. Polym. Sci.* **1996**, *62* (9), 1361−1376.

(19) Rolland, J. P.; Chen, K.; Poelma, J.; Goodrich, J.; Pinschmidt, R.; et al., 2015. Methods of producing polyurethane three-dimensional objects from materials having multiple mechanisms of hardening. US Patent No. WO2015/200179.

(20) Wang, G.; Peng, L.; Zheng, Y.; Gao, Y.; Wu, X.; Ren, T.; Gao, C.; Han, J. Novel Triethylamine Catalyzed S → O Acetyl Migration Reaction to Generate Candidate Thiols for Construction of Topological and Functional Sulfur-Containing Polymers. *RSC Adv.* **2015**, *5* (8), 5674−5679.

(21) Wojdyr, M. Fityk: A General-Purpose Peak Fitting Program. *J. Appl. Crystallogr.* **2010**, *43* (5), 1126−1128.

(22) Kulkarni, S. S.; Sayers, J.; Premdjee, B.; Payne, R. J. Rapid and Efficient Protein Synthesis through Expansion of the Native Chemical Ligation Concept. *Nat. Rev. Chem.* **2018**, *2*, No. 0122.

(23) Dawson, P. E.; Kent, S. B. H. Synthesis of Native Proteins by Chemical Ligation. *Annu. Rev. Biochem.* **2000**, *69* (3), 923−960.

(24) Hemu, X.; Taichi, M.; Qiu, Y.; Liu, D. X.; Tam, J. P. Biomimetic Synthesis of Cyclic Peptides Using Novel Thioester Surrogates. *Biopolymers* **2013**, *100* (5), 492−501.

(25) Bender, M. L. Enhanced Rates of Acyl Transfer to a Neighboring Hydroxyl Group. *Bioorg. Chem.* **1975**, *4*, 84−92.

(26) Jin, H.; Lee, J.; Shi, H.; Lee, J. Y.; Yoo, E. J.; Song, C. E.; Ryu, D. H. Bioinspired Synthesis of Chiral 3,4-Dihydropyranones via S-to-O Acyl-Transfer Reactions. *Org. Lett.* **2018**, *20* (6), 1584−1588.

(27) Bezer, S.; Matsumoto, M.; Lodewyk, M. W.; Lee, S. J.; Tantillo, D. J.; Gagné, M. R.; Waters, M. L. Identification and Optimization of Short Helical Peptides with Novel Reactive Functionality as Catalysts for Acyl Transfer by Reactive Tagging. *Org. Biomol. Chem.* **2014**, *12* (9), 1488−1494.

(28) Martin, R. B.; Hedrick, R. I. Intramolecular S-O and S-N Acetyl Transfer Reactions. *J. Am. Chem. Soc.* **1962**, *84* (1), 106−110.

(29) Aksakal, S.; Aksakal, R.; Becer, C. R. Thioester Functional Polymers. *Polym. Chem.* **2018**, *9* (36), 4507−4516.

(30) Macková, H.; Plichta, Z.; Hlídková, H.; Sedláček, O.; Konefal, R.; Sadakbayeva, Z.; Dušková-Smrčková, M.; Horák, D.; Kubinová, Š. Reductively Degradable Poly(2-Hydroxyethyl Methacrylate) Hydrogels with Oriented Porosity for Tissue Engineering Applications. *ACS Appl. Mater. Interfaces* **2017**, *9* (12), 10544−10553.

(31) Byler, K. G.; Li, Y.; Houghten, R. A.; Martinez-Mayorga, K. The Role of Imidazole in Peptide Cyclization by Transesterification: Parallels to the Catalytic Triads of Serine Proteases. *Org. Biomol. Chem.* **2013**, *11* (18), 2979−2987.

(32) Law, S. K. A.; Dodds, A. W. The Internal Thioester and the Covalent Binding Properties of the Complement Proteins C3 and C4. *Protein Sci.* **1997**, *6* (2), 263−274.

(33) Nair, D. P.; Cramer, N. B.; McBride, M. K.; Gaipa, J. C.; Shandas, R.; Bowman, C. N. Enhanced Two-Stage Reactive Polymer Network Forming Systems. *Polymer* **2012**, *53* (12), 2429−2434.

(34) Zhang, X.; Xi, W.; Huang, S.; Long, K.; Bowman, C. N. Wavelength-Selective Sequential Polymer Network Formation Controlled with a Two-Color Responsive Initiation System. *Macromolecules* **2017**, *50* (15), 5652−5660.

(35) Meng, Y.; Jiang, J.; Anthamatten, M. Shape Actuation via Internal Stress-Induced Crystallization of Dual- Cure Networks. *ACS Macro Lett.* **2015**, *4*, 115−118.

DOI: 10.1021/acs.macromol.9b01678
Macromolecules 2019, 52, 8114−8123

(36) Anthamatten, M.; O'Neill, S. W.; Liu, D.; Wheler, T. M.; Vallery, R. S.; Gidley, D. W. Tunability of Free Volume and Viscoelastic Damping of Thiol − Ene Networks Deep in the Glassy State. *Macromolecules* **2018**, *51*, 2564−2571.

DOI: 10.1021/acs.macromol.9b01678
Macromolecules 2019, 52, 8114−8123